Reprints from
Gordon and Breach

# MECHANISM OF CLASSIFICATION IN A STURTEVANT-TYPE AIR CLASSIFIER

G. JIMBO, M. YAMAZAKI, J. TSUBAKI and T.S. SUH

*Department of Chemical Engineering, Nagoya University, Furo-cho, Chikusa-ku, Nagoya 464, Japan*

*Chem. Eng. Commun.* Vol. 34 pp. 37–48
0098-6445/85/3401–0037$20.00/0


# MECHANISM OF CLASSIFICATION IN A STURTEVANT-TYPE AIR CLASSIFIER

G. JIMBO, M. YAMAZAKI, J. TSUBAKI and T.S. SUH

*Department of Chemical Engineering, Nagoya University, Furo-cho, Chikusa-ku, Nagoya 464, Japan*

(*Received November 14, 1983; in final form May 30, 1984*)

The estimation of air velocity distributions and particle trajectories is inevitable to analyse the mechanism of classification, but the direct measurement of it is extremely difficult.

The authors, here report three dimensional air velocity distributions within the inside drum of a model Sturtevant-type air classifier measured by a spherical five-holed Pitot-tube, and also two dimensional particle ejecting velocities on a model distributor determined by photography.

Using those results, the cut size calculated from particle trajectories in the classifier is compared with the experimental results and theoretical values.

KEYWORDS Classification Sturtevant-type classifier

## INTRODUCTION

The Sturtevant- and the Gayco-type air classifiers have widely been used in cement and other industries, yet the set-up of the classifiers are so complicated that both the air flow and the particle trajectory in it have so far not been clearly understood.[1,2,4,6]

The cut size is an important characteristic for the evaluation of the classifier performance. Tanaka *et al.*[7] made an analysis to calculate the cut size of the Gayco-type air classifier assuming the tangential velocity of particles ejected at the distributor is same as the circumferential speed of the distributor, and particles move up with the same velocity of air in the axial direction, further particles reached the wall of the inside drum during their residence time fall down into the coarse. On the other hand, Gotō[2] calculated the cut size and the fractional recovery curves of the Sturtevant-type air classifier and obtained the relation between particle size and separation efficiency of the auxiliary blades assuming collided particles against the blades fall down into the coarse.

To get a more accurate classification mechanism, the authors measured the three dimensional air velocity distributions within the inside drum of a model Sturtevant-type air classifier by a spherical five-holed Pitot-tube. Also, two dimensional particle velocities on a model distributor were determined by photography.

Using those results, particle trajectories are precisely calculated and the obtained cut size has shown a good agreement with the experimental results.

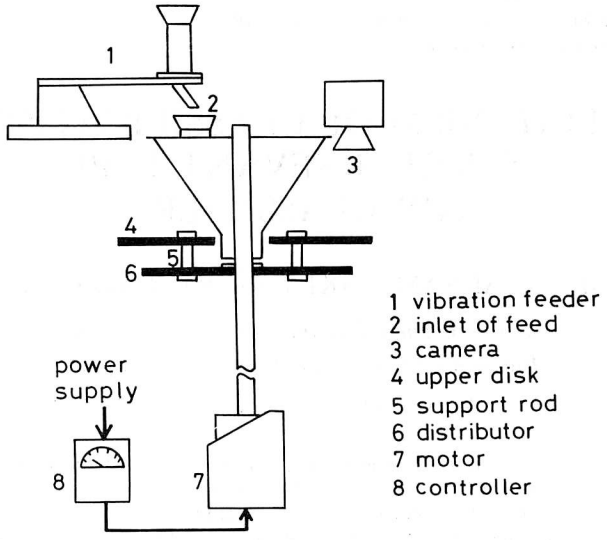


FIGURE 1 Schematic diagram of a model distributor with an upper disk of plexiglas which is removable.

## I. MATERIALS AND METHOD

### *1. Experimental Apparatus and Procedure*

The schematic diagram of the model distributor is shown in Figure 1. Powders seep out from the gap under the chute, then spread out through the openings of eight support rods (5). Here, a pair of axially symmetrical openings are selected in order to get a clear particle trace, and the remaining openings are blinded. An upper disk (4) of plexiglas simulates a plate which fixes auxiliary blades. In both cases, photographs are taken with and without upper disk. Here we will discuss the latter case only.

An example of the trace of fused alumina powders ($\bar{d}_p \fallingdotseq 67\ \mu$m) on the model distributor rotating at 126 rad/s (1200 rpm) is shown in Figure 2. Here, the particle trace is called a broad band which consists of ejected particles. The width of this trace was controlled by setting shutter speed of the camera from 1/400 second to 1/250 second.

The rotating speed of the distributor and the feed rate of powder were selected as operating variables. Fused alumina powder of average size of 67 $\mu$m was used as the feed material.

Classification experiments were run using fused alumina powders at 105 rad/s (1000 rpm). The observed cut size was 52 $\mu$m, which is smaller than the calculated value.

### *2. Calculation of Particle Velocity*

The direction of the particles as they came out from the exit gap between two support rods was seen as nearly a straight line on the distributor, as shown in Figure 2.

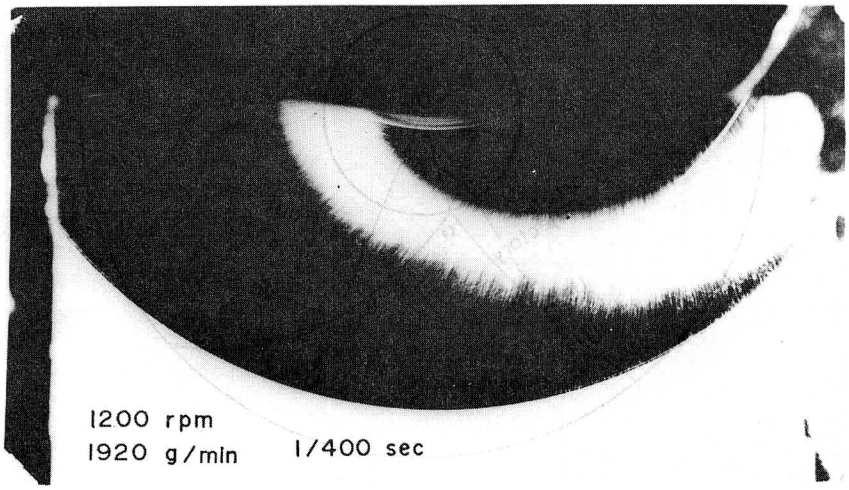


FIGURE 2 Photograph of particle trace of fused alumina powder on the model distributor at 1200 rpm.

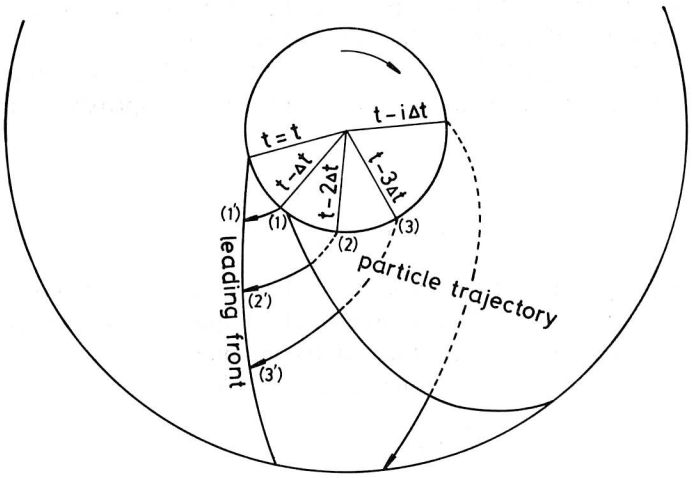


FIGURE 3 Sketch of a particle trace on the rotating distributor.

However, since the distributor is in rotating motion, the actual particle path is taken as a type of envelope. We have named this envelope the leading front.

An example of a particle trace sketch on the distributor is shown in Figure 3. A particle came out from opening (1) at time $\Delta t$ before time $t$ went to position (1′), and a particle came out from opening (2) at time $2\,\Delta t$ before time $t$ went to position (2′), when the photograph was taken at time $t$. From Figure 3, it is known that the leading front indicates the relative motion between particles and the distributor.

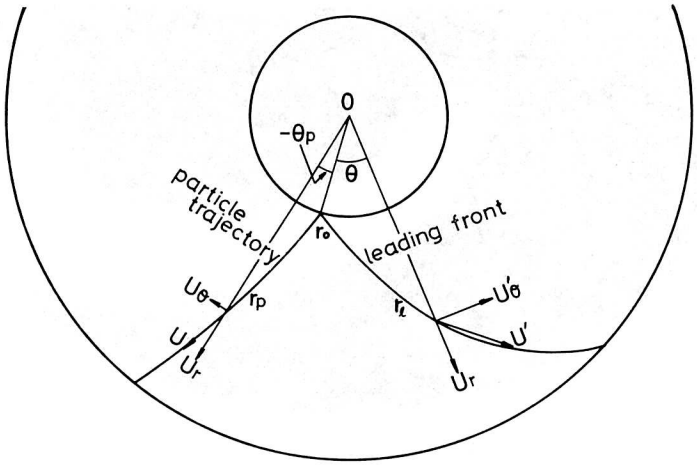


FIGURE 4 Relation between the leading front and the particle trajectory.

The particle trajectory must just be determined in order to calculate the motion of a particle on the distributor. For that purpose, a particle path is traced on a sheet of tracing paper which is placed coaxially on the photograph. When that tracing paper is rotated continuously, a particle trace as shown in Figure 4 can be synthesized.

Point $r_l$ on the leading front and $r_p$ on the trace are well approximated by following equations.

$$r_l = r_0 + a_l \theta_l^{k_l} \tag{1}$$

$$r_p = r_0 + a_p |-\theta_p|^{k_p} \tag{2}$$

where, $r_0$ is initial position of particles, and $a_l$, $k_l$, $a_p$, and $k_p$ are all constants.

Let $u_r$ and $u_\theta$ be the radial and tangential components of particle velocity $\vec{u}$, respectively. Further, since $u'_\theta$ is the tangential component of relative particle velocity $\vec{u}'$ against the distributor, the following equations hold.

$$u'_\theta = u_\theta - u_{d\theta} \tag{3}$$

$$\frac{u_r}{u'_\theta} = \frac{\dot{r}_l}{r_l \dot{\theta}_l} = \frac{1}{r_l} \frac{dr_l}{d\theta_l} \tag{4}$$

$$\frac{u_r}{u_\theta} = \frac{\dot{r}_p}{r_p \dot{\theta}_p} = \frac{1}{r_p} \frac{dr_p}{d\theta_p} \tag{5}$$

where, $u_{d\theta}$ is the tangential velocity of the distributor.

Equations (3), (4), and (5) can be solved simultaneously by using Eqs. (1) and (2). Thus, $\vec{u}$ at point $r_p$ and its components $u_r$ or $u_\theta$ are all determined by knowing $u_{d\theta}$, $dr_l/d\theta_l$, and $dr_p/d\theta_p$, where $dr_l/d\theta_l$ and $dr_p/d\theta_p$ are slopes of the leading front and the particle trajectory, respectively.

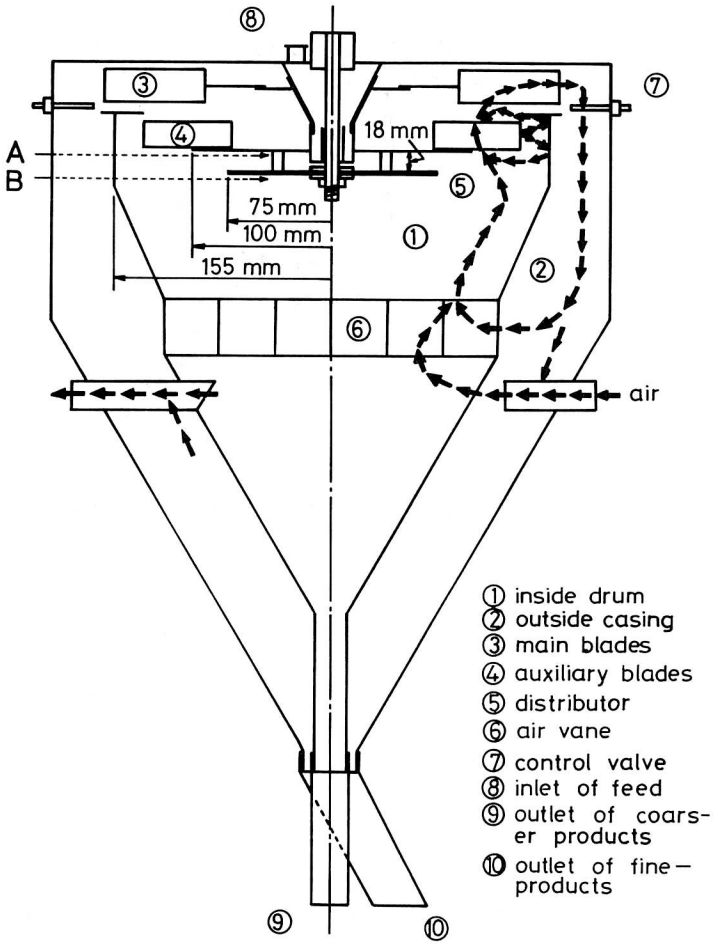


FIGURE 5 Schematic diagram of the model Sturtevant-type air classifier.

## II. RESULTS AND DISCUSSION

### *1. Distributions of Air Velocity within a Model Classifier*

Though the estimation of the particle trajectories is mandatory to the analysis of the mechanism of classification, the direct measurement of it is impossible. Therefore, for such an estimation, the equations of motion of a particle are numerically solved under certain special conditions.

The schematic diagram of the Sturtevant-type model classifier used in this experiment is shown in Figure 5. It consists mainly of an inside drum (1), an outside casing (2), main blades (3), auxiliary blades (4) and a distributor (5) which rotates with

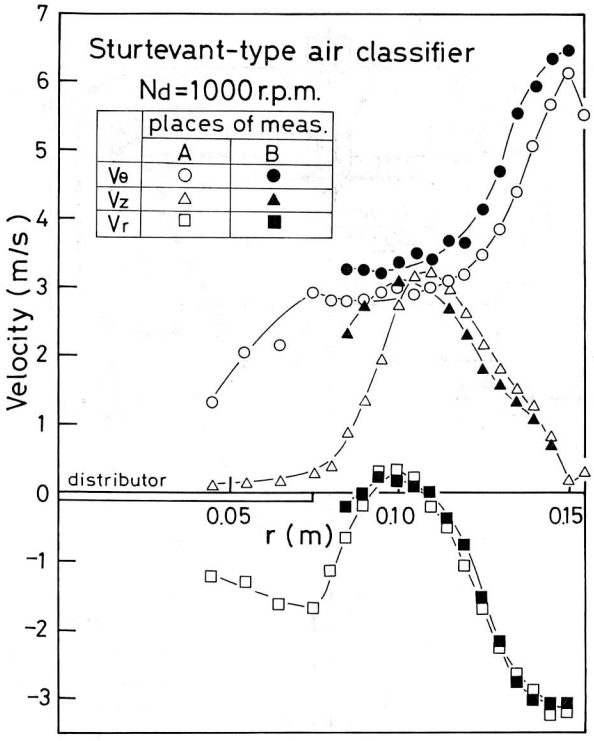


FIGURE 6 Three dimensional air velocity distributions within the inside drum of the model classifier with 8 main blades and 40 auxiliary blades at 1000 rpm.

the shaft. Feed particles scattered on the distributor are influenced by the auxiliary blades. Particles that escaped the action are carried out with the circulating air flow and are discharged from the outside casing as fines.

Air flow is measured along the line (*A*) under the auxiliary blades and along the line (*B*) just under the distributor. The velocity distributions of air are measured by a spherical five-holed Pitot-tube of 5 mm diameter, which travels radially from 45 mm to 155 mm from the axis of the classifier.

A result of the velocity distributions of air flow inside drum[5] is shown in Figure 6. Tangential, axial, and radial velocities of air are shown here as $v_\theta$, $v_z$, and $v_r$,respectively. The radial velocity of air is almost negative and it will be discussed later.

## 2. *Particle Velocity*

It was extremely difficult to measure the particle velocity in the classifier. Therefore, we made a model distributor which has the same size of the model classifier, and measured the particle velocity on the distributor using a camera.

Particle ejecting velocities at the edge of the distributor ($r_d = 0.075$ m) are summarized in Figure 7. Both the radial and tangential particle velocities at the circumference of the distributor increase linearly against the rotating speed, and the

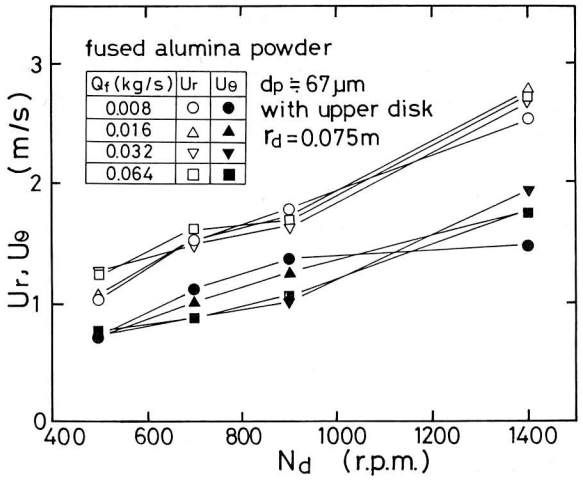


FIGURE 7 Particle ejecting velocities of fused alumina powder on the rotating distributor with upper disk.

effect of the feed rate seems to be small. Therefore, the average particle velocity is adopted in the calculation of the particle trajectory in the classifier.

The tangential velocity ratio $u_\theta/u_{d\theta}$ of particles to the distributor at its edge is shown in Figure 8. It shows a large slip velocity between particles and the distributor, but $u_\theta/u_{d\theta}$ values themselves are not so much affected with $N_d$ nor $Q_f$. In fact, the ratio of $u_\theta/u_{d\theta}$ is significant and the cut size is greatly changed by the ratio. In their theoretical analysis, Tanaka *et al.*[7] assumed that the value of $u_\theta/u_{d\theta}$ is unity, but it is now clear that it has to be assumed to be between 0.1 and 0.2. This is thought to be the reason for the large deviation of Tanaka's equation from experimental data. This will be discussed later.

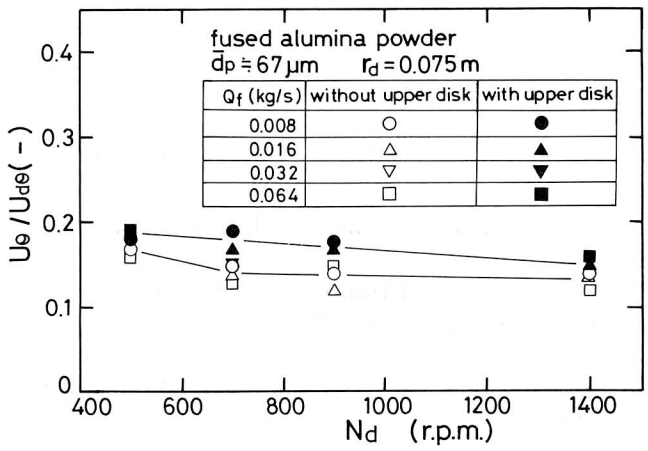


FIGURE 8 Ratio of the tangential velocity of particles to the circumferential velocity of distributor.

*3. Calculation of Particle Trajectory in the Classifier*

We experimentally obtained both the air velocity distribution in the inside drum and the particle ejecting velocity at the distributor. Therefore, we could determine the cut size from the particle trajectory, solving the equations of motion of a particle numerically.

Since the shape of the chamber in the Sturtevant-type air classifier is cylindrical, particle motion inside the chamber is represented by cylindrical coordinates.

The equations of motion of a particle can be represented in vectorial form as follow:

$$m\vec{a} = C_D \cdot S\left(\frac{1}{2}\rho_f|\vec{V}|\vec{V}\right) + \vec{F} \tag{6}$$

where, $m$, $\vec{a}$, $S$, $\vec{V}$, and $\vec{F}$ are mass, acceleration, projected area, relative air velocity, and external force on a particle, respectively.

Odar's equation is adopted for the drag coefficient $C_D$ because of its wide applicability of particle Reynolds number, even up to Reynolds number 1000.

$$C_D = \frac{24}{Re}(1 + 0.125\, Re^{0.72}) \tag{7}$$

where,
$$Re = \frac{d_p|\vec{V}|\rho_f}{\mu}, \quad \vec{V} = \vec{v} - \vec{u}$$

and
$$|\vec{V}| = \sqrt{(v_r - u_r)^2 + (v_\theta - u_\theta)^2 + (v_z - u_z)^2}$$

Here, $d_p$, $\rho_f$, $\vec{v}$, and $\vec{u}$ are particle diameter, air density, air velocity, and particle velocity, respectively.

Particle motion in the model classifier can be described in cylindrical coordinates as follows:

$$\ddot{r} - r\dot{\theta}^2 = \frac{18\mu}{\rho_p d_p^2}(v_r - \dot{r})(1 + 0.125\, Re^{0.72}) \tag{8}$$

$$r\ddot{\theta} + 2\dot{r}\dot{\theta} = \frac{18\mu}{\rho_p d_p^2}(v_\theta - r\dot{\theta})(1 + 0.125\, Re^{0.72}) \tag{9}$$

$$\ddot{z} = \frac{18\mu}{\rho_p d_p^2}(v_z - \dot{z})(1 + 0.125\, Re^{0.72}) - g \tag{10}$$

In this case, gravity acts as an external force in the $z$-direction. Therefore, the gravity constant $g$ is added in Eq. (10).

Equations (8), (9) and (10) are numerically calculated by Runge–Kutta method using a particle ejecting velocity $\vec{u}_0$ at the edge of the distributor and the observed air velocity $\vec{v}(r)$ which is independent of $z$ within the inside drum. Here, velocity distributions of air are read by a digitizer, and values at every 1 mm radial positions are interpolated by parabolic approximation.

In computation, the data of air velocity is assumed to be along the line ($A$) in Figures 5 or 6 and the time increment is assumed to be 0.0025 second.

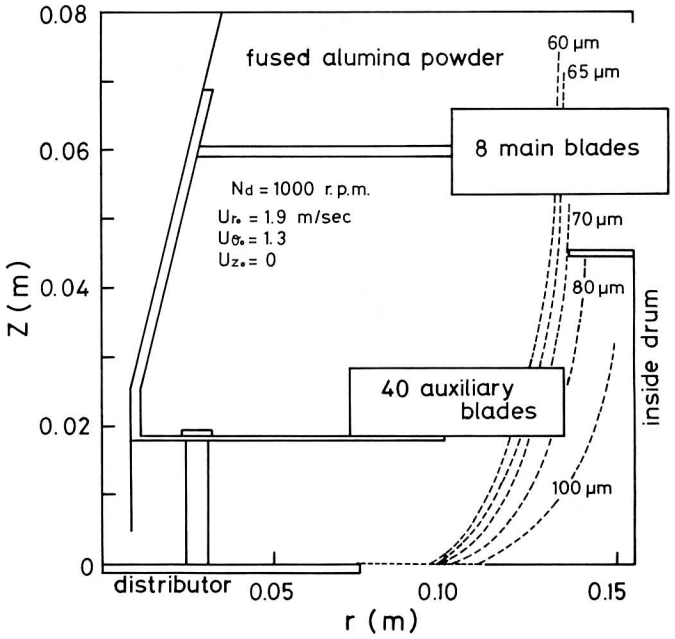


FIGURE 9 Vertical trajectories of particles ejected at the edge of the model distributor (at $N_d = 1000$ rpm, $r_d = 0.075$ m).

### 4. *Calculation of Cut Size*

Vertical and horizontal particle trajectories in the inside drum of the model classifier are shown in Figures 9 and 10, respectively, for every particle size. A particle ejected at the edge of the distributor flies almost horizontally and moves up gradually by the ascending air flow which was caused by main blades at the top. Particles traveling in this manner are greatly affected by the ejecting velocity at the distributor, and the trajectory of a particle changes greatly by the ejecting velocity. Here, the cut size $d_{p50}$ is defined as the particle which touches the circumference of the inside drum cover. Particles larger than 70 $\mu$m fall down as coarse fraction, and particles finer than 70 $\mu$m will move up and discharge as fines.

### 5. *Comparison of Calculated and Observed Values*

So far, we have calculated the particle trajectory in a model classifier, and the differences between the calculated and observed values is discussed.

Results of the calculated and observed cut size are shown in Figure 11. The lower line is an estimation by Tanaka's equation, and the upper one is an estimation by Gotō's equation.

Though the calculated cut size gives somewhat larger value than the observed one as mentioned before, the dependence on the rotating speed is almost similar for both cases, as the inclination of the two lines shows. However, the theoretical cut size as estimated by Tanaka's or Gotō's equation gives not only a larger deviation from

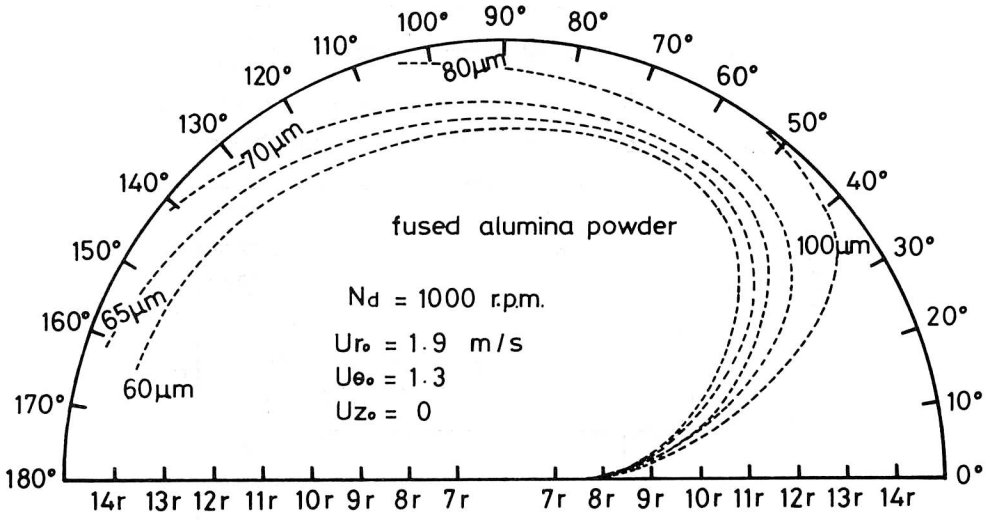


FIGURE 10 Horizontal particle trajectories.

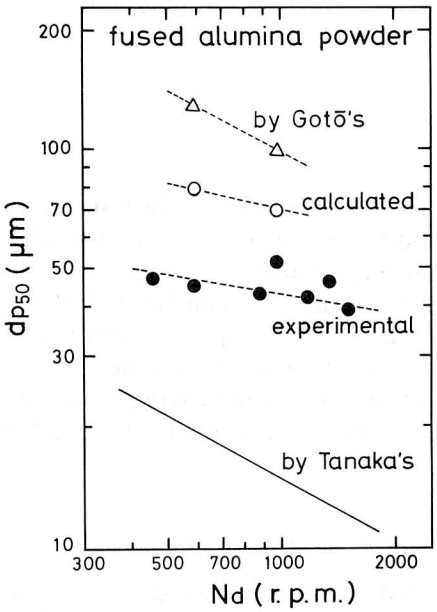


FIGURE 11 Comparison among calculated and observed cut sizes.

observed values, but also steeper inclination against the rotating speed. And from those facts, our results are somewhat improved over results derived from the two previous methods.

One possible reason for our observation of values lower than the calculated values is perhaps the lack of data on the air velocity near the auxiliary blades. As mentioned

before, the air velocity is measured between the auxiliary blades and the distributor. We could not measure the secondary air flow into the blades because of the limit of our measuring technique. Therefore, it seems that the radial air flow was estimated too low, which makes the calculated cut size higher.

On the other hand, the cut size estimated by Tanaka's model[7] gives a lower value, and this is due to the assumption of the tangential velocity of particle. He assumed that particles travel the inside drum with the same velocity as the circumferential speed of the distributor. But it is now clear that this assumption was an over estimation, and it makes the cut size of the fines smaller. Further, the cut size estimated by Gotō's model[2] gives a larger value than is observed. He assumed the particle velocity at the edge of the distributor to be negligible, and took into account only the axial velocity of air. This would be the cause of the larger cut size of fines.

If the secondary flow into the auxiliary blades could be taken into account, the estimation of cut size would become more accurate.

## III. SUMMARY AND CONCLUSIONS

1) Three dimensional air velocity distributions within a model Sturtevant-type air classifier are presented.
2) A new method of measuring two dimensional particle velocity on the rotating model distributor has been presented.
3) Three dimensional particle trajectory within the model classifier are numerically solved using particle ejecting velocity and air velocity distribution.
4) Cut size calculated from particle trajectories in the classifier has shown a better agreement with the experimental values than the results by Tanaka or Gotō.

## NOMENCLATURE

| | |
|---|---|
| $a_l$, $a_p$ | constants in Eqs. (1) and (2) |
| $\vec{a}$ | acceleration in Eq. (6), m/s$^2$ |
| $C_D$ | drag coefficient |
| $d_p$ | particle diameter, m |
| $d_{p50}$ | cut size, m |
| $\bar{d}_p$ | volume mean diameter, m |
| $\vec{F}$ | external force, $N$ |
| $g$ | acceleration of gravity, m/s$^2$ |
| $k_l$, $k_p$ | constants in Eqs. (1) and (2) |
| $m$ | mass of a particle, kg |
| $N_d$ | rotating speed of the distributor, rad/s |
| $Q_f$ | feed rate, kg/s |
| $Re$ | particle Reynolds number |

| | |
|---|---|
| $r$ | radius in the classifier, m |
| $r_0$ | initial particle position on the distributor, m |
| $r_d$ | radius of the distributor, m |
| $r_l$, $r_p$ | radial particle position on the distributor, m |
| $S$ | projected area of a particle, $m^2$ |
| $t$ | time, s |
| $\vec{u}$ | particle velocity, m/s |
| $u_0$ | initial particle velocity, m/s |
| $u_{d\theta}$ | tangential velocity of the distributor, m/s |
| $u_r$ | radial component of $\vec{u}$, m/s |
| $u_\theta$ | tangential component of $\vec{u}$, m/s |
| $u_z$ | axial component of $\vec{u}$, m/s |
| $\vec{u}'$ | relative velocity of a particle to the distributor, m/s |
| $u'_\theta$ | tangential component of $\vec{u}'$, m/s |
| $\vec{V}$ | relative air velocity, m/s |
| $\vec{v}$ | air velocity, m/s |
| $v_r$ | radial component of $\vec{v}$, m/s |
| $v_z$ | axial component of $\vec{v}$, m/s |
| $v_\theta$ | tangential component of $\vec{v}$, m/s |
| $z$ | height above the distributor, m |
| $\theta$ | angle in the cylindrical coordinates, deg |
| $\theta_l$ | angle of delay of a particle on the distributor, deg |
| $\theta_p$ | angle of rotation of a particle on the distributor, deg |

REFERENCES

1. Burson, J.H., III, Keng, E.Y.H., and Orr, Jr., C., *Powd. Technol.*, **1,** 305 (1967/68).
2. Gotō, K., *Cement Gijutsu Nempō* (Proceedings of Japan Cement Engineering Association, Japan), **13,** 102 (1959).
3. Iinoya, K., and Kimura, N., *Kikai no Kenkyū* (Science of Machine, Japan), **3,** 600 (1951).
4. Jimbo, G., Suh, T.S., Tsubaki, J., and Yamazaki, M., *J. Soc. Powder Tech. Japan*, **10,** 576 (1982).
5. Jimbo, G., Yamazaki, M., and Koike, T., *KagakuKogaku Ronbunshu* (in press).
6. Onuma, E., *J. Chem. Eng. Japan*, **6,** 527 (1973).
7. Tanaka, T., Kuwano, K., and Kawai, S., *Kagaku Kōgaku* (Chemical Engineering, Japan), **21,** 798 (1957).